The EMBO Journal Vol.16 No.12 pp.3455–3463, 1997

Tetramerization of the AKT1 plant potassium channel involves its C-terminal cytoplasmic domain

Pierre Daram, Serge Urbach, Frédéric Gaymard, Hervé Sentenac and Isabelle Chérel[1]

Laboratoire de Biochimie et Physiologie Moléculaire des Plantes, ENSA-M/INRA/CNRS URA 2133/UM2, 34060 Montpellier cedex 01, France

[1]Corresponding author

All plant channels identified so far show high conservation throughout the polypeptide sequence except in the ankyrin domain which is present only in those closely related to AKT1. In this study, the architecture of the AKT1 protein has been investigated. AKT1 polypeptides expressed in the baculovirus/*Sf*9 cells system were found to assemble into tetramers as observed with animal Shaker-like potassium channel subunits. The AKT1 C-terminal intracytoplasmic region (downstream from the transmembrane domain) alone formed tetrameric structures when expressed in *Sf*9 cells, revealing a tetramerization process different from that of Shaker channels. Tests of subfragments from this sequence in the two-hybrid system detected two kinds of interaction. The first, involving two identical segments (amino acids 371–516), would form a contact between subunits, probably via their putative cyclic nucleotide-binding domains. The second interaction was found between the last 81 amino acids of the protein and a region lying between the channel hydrophobic core and the putative cyclic nucleotide-binding domain. As the interacting regions are highly conserved in all known plant potassium channels, the structural organization of AKT1 is likely to extend to these channels. The significance of this model with respect to animal cyclic nucleotide-gated channels is also discussed.

Keywords: *Arabidopsis thaliana*/baculovirus/potassium channel/tetramerization/two-hybrid system

Introduction

Plant potassium channels form a growing family of homologous proteins. Since the initial cloning of *AKT1* (Sentenac *et al*., 1992) and *KAT1* (Anderson *et al*., 1992) *Arabidopsis thaliana* cDNAs by functional complementation of yeast mutants, four new cDNAs coding for plant channels have been reported, two from *Arabidopsis*: *AKT2/AKT3* (Cao *et al*., 1995; Ketchum, 1996) and *KAT2* (unpublished, DDBJ/EMBL/GenBank accession number: U25695) and two from potato (*Solanum tuberosum*), *KST1* (Müller-Röber *et al*., 1995) and *SKT1* (DDBJ/EMBL/GenBank accession number X86021). All of them comprise, from their N-terminal to their C-terminal ends: a short hydrophilic region, a hydrophobic region structurally analogous and partially homologous to the transmembrane domain of voltage-gated animal channels from the Shaker superfamily (Jan and Jan, 1992), a putative cyclic nucleotide-binding domain, and a conserved C-terminal end of unknown function. Between these last two regions, some of them (AKT1, AKT2 and SKT1) contain an ankyrin-repeat domain with six repeats homologous to those of human erythrocyte ankyrin (Lux *et al*., 1990). Ankyrin repeats are found in a large variety of proteins, and have been shown to be involved in protein–protein interactions (Michaely and Bennett, 1992). Recently, ankyrin repeats have been reported in a *Drosophila* plasma membrane calcium channel (Wes *et al*., 1995). The role of such motifs in channels is still unknown.

The closest known relatives of plant channels are voltage-gated potassium channels which belong to the Shaker superfamily (Pongs, 1992) and cyclic nucleotide-gated channels (Zufall *et al*., 1994). Detailed data concerning protein structure and assembly are available for Shaker-like channels. A tetrameric organization was proposed for these potassium channels, by analogy with sodium and calcium channels, which are composed of four tandemly associated homologous domains, each similar to a Shaker cDNA product (Caterall, 1995). Experimental evidence for association between subunits was obtained by coexpression in *Xenopus* oocytes of cDNAs from different subfamilies of voltage-gated potassium channels (Isacoff *et al*., 1990; Ruppersberg *et al*., 1990; Li *et al*., 1992). A stoichiometry of four subunits per channel protein was deduced thereafter from the properties of heteromultimeric channels formed by the association of wild type and mutant toxin-resistant subunits (MacKinnon, 1991) and from the expression of multimeric constructs (Liman *et al*., 1992). Electron microscopy images of purified Shaker proteins revealed a symmetrical tetrameric complex organized around a central vestibule (Li *et al*., 1994).

In voltage-gated Shaker-type channels, a domain involved in subunit assembly, located in the N-terminal region, was identified by deletion experiments combined with biochemical approaches (Li *et al*., 1992; Shen *et al*., 1993) or with electrophysiological studies (Li *et al*., 1992; Hopkins *et al*., 1994). This domain is capable of self-assembly (Li *et al*., 1992; Shen *et al*., 1993; Pfaffinger and DeRubeis, 1995) and is responsible for subfamily-specific recognition between subunits (Li *et al*., 1992; Shen *et al*., 1993; Shen and Pfaffinger, 1995; Xu *et al*., 1995). It also seems to be absolutely required for subunit assembly of a Kv1.1 channel (Shen *et al*., 1993). However, in Kv1.5 (Attali *et al*., 1993), Kv1.4 (Lee *et al*., 1994) and Kv1.3 channels (Tu *et al*., 1995, 1996), this domain can be removed without leading to disappearance of currents measured in *Xenopus* oocytes, thus confirming the earlier results of Van Dongen *et al*. (1990) who

observed that deletions removing N- and C-terminal hydrophilic parts did not prevent the formation of functional Kv2.1 channels. This correlates with results obtained in dominant-negative experiments in oocytes, where coexpression of the tetramerization domain with wild type subunits has been observed to have a strong effect on channel activity in the case of a Kv1.1 channel (Li *et al.*, 1992; Babila *et al.*, 1994) but no significant effect for Kv1.3 or Kv1.5 channels (Babila *et al.*, 1994; Tu *et al.*, 1995). Differences in channel isoform properties could explain these discrepancies (Tu *et al.*, 1996). In agreement with the assumption that interactions occur inside the hydrophobic core, the first transmembrane segment (S1) was shown to play an important role in Shaker channel oligomerization (Shen *et al.*, 1993; Babila *et al.*, 1994), and experiments performed with a mouse Kv1.3 channel revealed the participation of other segments (probably S2, S3 and S4) (Tu *et al.*, 1996). The four H5 regions also associate in a hydrophobic environment to form the pore of the channel (Kirsch *et al.*, 1993; Peled and Shai, 1993). It has been suggested (Babila *et al.*, 1994) that the conserved N-terminal sequences would drive specific recognition between subunits and their assembly in the cytoplasm, while interactions between hydrophobic regions would stabilize the complex in the membrane.

In plant K^+ channels, there is no equivalent of the N-terminal region of voltage-gated animal channels. The similarity between AKT1 and voltage-gated Shaker channels is restricted to the hydrophobic domain, which displays a common structural design (six transmembrane segments, a H5 sequence forming the pore between S5 and S6, and the S4 segment forming the voltage sensor), whereas homology to cyclic nucleotide-gated channels covers a larger region from the first transmembrane segment to the end of the cyclic nucleotide-binding domain. Although the high degree of conservation found between H5 regions of all potassium channels suggests a common arrangement of the pore, the spatial organization of plant channel subunits remained unresolved.

This paper concerns the organization of the channel AKT1. This channel is expressed in the surface tissue of roots and is probably involved in K^+ uptake from the soil solution (Lagarde *et al.*, 1996). AKT1 is functional and behaves as an inwardly rectifying voltage-gated channel when expressed in *Sf*9 insect cells using a recombinant baculovirus (Gaymard *et al.*, 1996). However, it has not been possible to detect any associated current for this channel, or its homologue AKT2 which also possesses an ankyrin domain (Cao *et al.*, 1995), in the *Xenopus* oocyte expression system. In order to study AKT1 structure, we developed a strategy using two different approaches: biochemical analysis of the purified protein, and two-hybrid system experiments. Unlike animal channels, AKT1 has a short hydrophilic N-terminus (60 amino acids), but displays a very long peptide sequence (562 amino acids) downstream from the last transmembrane segment. Our results support evidence for a tetrameric structure of the protein, and show that this long C-terminal region is by itself able to form a tetramer *in vitro*. Experiments using the two-hybrid system have delineated the structural elements responsible for the interactions. A central role for the large region, located in AKT1 between the hydrophobic domain and the ankyrin repeats, was revealed. This region is conserved in all known plant potassium channels as well as animal cyclic nucleotide-gated channels.

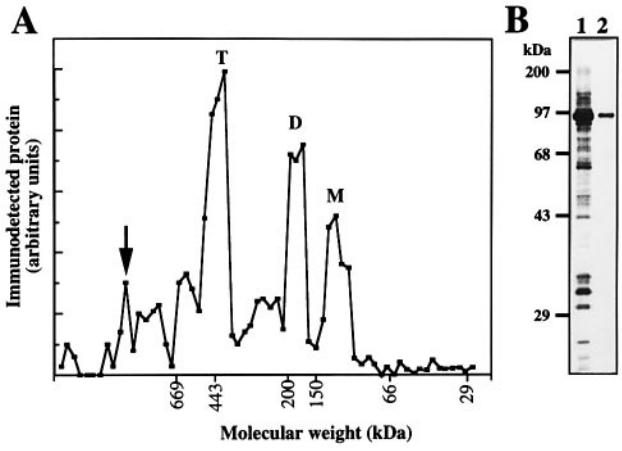

Fig. 1. Size-exclusion chromatography of the AKT1 protein. (**A**) Elution profile of AKT1 polypeptides after size-exclusion chromatography. Fractions of 0.25 ml were collected. Proteins of molecular weights corresponding to an AKT1 tetramer (T), dimer (D) and monomer (M) are indicated on the figure. The exclusion volume is marked by an arrow. The AKT1 polypeptide was quantified in each fraction by dot blot analysis and scanning of the photographic film. (**B**) SDS–polyacrylamide gel (silver nitrate staining) showing the extract used for loading, where AKT1 was partially purified by anion exchange chromatography (lane 1) and the AKT1 protein in the tetramer peak fraction (lane 2).

Results

AKT1 assembly

Production of the AKT1 protein in *Sf*9 cells has been described previously (Gaymard *et al.*, 1996). AKT1 was solubilized from the microsomal fraction of *Sf*9 cells with lysophosphatidylcholine, and partially purified using an anion-exchange column. In order to obtain an estimate of the molecular weight of AKT1, the purified polypeptide was loaded onto a size-exclusion column (Sephacryl S-300, Pharmacia). The chromatography was carried out under non-denaturing conditions in the presence of lysophosphatidylcholine. An aliquot of each eluted fraction was tested by dot blot with an anti-AKT1 serum, and spot intensities were quantified by densitometry. The elution profile revealed three peaks (Figure 1A). The highest one corresponded to a complex whose molecular weight was estimated to range between 385 and 425 kDa, consistent with that expected for a tetramer of identical 95 kDa subunits. To eliminate the possibility that the elution of AKT1 as a high molecular weight complex resulted from its association with other proteins, the peak fraction was analysed by SDS gel electrophoresis. After silver nitrate staining of the gel, only the 95 kDa AKT1 polypeptide was detectable (Figure 1B). The other two peaks could be ascribed to the presence of a dimer (mol. wt 173–213 kDa) and a monomer (81–121 kDa).

Assembly of the C-terminal cytoplasmic region of AKT1 (AKT1 C-Term)

AKT1 C-Term is defined as the sequence (supposed to be intracytoplasmic) lying downstream from the last transmembrane segment (ranging from H294 to the end of the polypeptide). A large amount of correctly folded

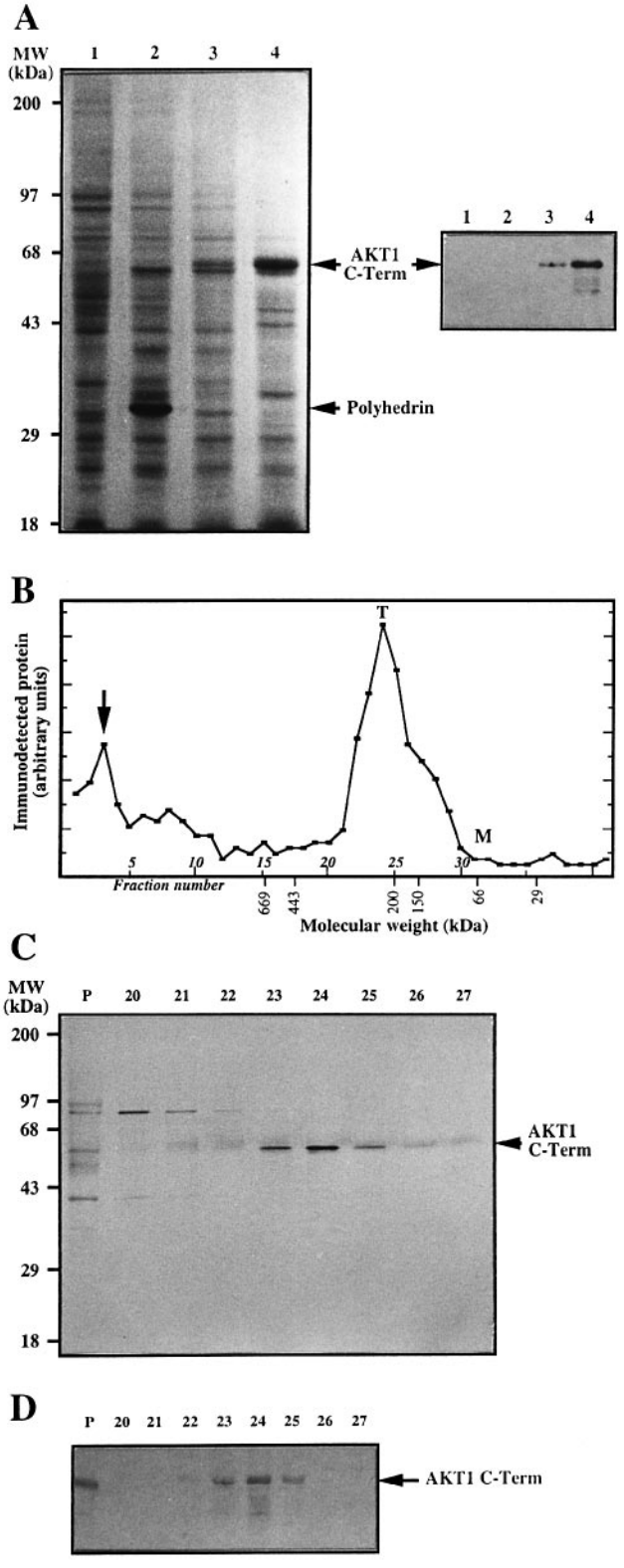

polypeptide was required for further analyses of its biochemical properties. For this reason, the baculovirus expression system was chosen, rather than production in *Escherichia coli*, because the polypeptide is denatured when expressed in bacteria (our unpublished data). The sequence coding for AKT1 C-Term was inserted into the baculovirus genome in place of the polyhedrin gene, by cotransfection of the wild type baculovirus DNA with the plasmid containing the cDNA sequence. The recombinant baculovirus was used to infect *Sf*9 cells. From these cells, a specific polypeptide, which after 2 days of infection constitutes the major band detectable on a Coomassie blue-stained SDS–polyacrylamide gel, was observed in the total soluble protein extract (Figure 2A, lanes 3 and 4). This polypeptide was not found in extracts of non-infected cells or in wild type baculovirus infected cells (Figure 2A, lanes 1 and 2). Its apparent molecular weight was consistent with that (~60 kDa) calculated for the peptide sequence of AKT1 C-Term. Furthermore, the Western blot analysis performed with the anti-AKT1 serum revealed only the 60 kDa band (Figure 2A, right).

An extract enriched in the 60 kDa polypeptide was obtained by chromatography of the *Sf*9 soluble protein on an ion exchange column. This extract was then fractionated by passing through a size-exclusion column. Dot blot analysis of the different fractions revealed a major peak which was maximal in fractions 23 and 24 corresponding to molecular weights from 230 to 245 kDa (Figure 2B). A shoulder on this peak was also present at ~120 kDa. No signal was detected for fractions corresponding to the monomer molecular weight (60 kDa). Electrophoretic analysis of the relevant peak fractions 20–27 revealed a few polypeptides. The 60 kDa AKT1 C-Term polypeptide was detected by silver nitrate staining and Western blot (Figure 2C and D). As a single 60 kDa band was observed in peak fractions 23 and 24 (Figure 2C), the most likely explanation for the elution profile shown in Figure 2B is that four identical AKT1 C-Term polypeptides assembled to form a 240 kDa homotetrameric complex. The 120 kDa shoulder visible on the chromatogram (Figure 2B) could correspond to a homodimeric form.

Delineation of the AKT1 domains involved in the interactions

The two-hybrid system was used to test the interactions between the various cytoplasmic domains present in the hydrophilic C-terminus of the protein. The sequence

Fig. 2. Production and molecular weight determination of the AKT1 C-Term protein complex. (**A**) Expression of AKT1 C-term in *Sf*9 cells. Left, SDS–polyacrylamide gel of soluble proteins of *Sf*9 cells (40 μg protein per lane, Coomassie blue staining). Lane 1, uninfected *Sf*9 cells; lane 2, cells infected with wild type baculovirus; lanes 3 and 4, cells infected with recombinant baculovirus and harvested after 24 h (3) or 48 h incubation (4). Right, Western blot analysis performed with the anti-AKT1 serum. Each lane of the gel contained 10 μg protein. (**B**) Size-exclusion chromatography of an AKT1 C-Term-enriched fraction. Each fraction corresponded to 0.5 ml. See Figure 1A for abbreviations. (**C**) Analysis of fractions 20 to 27 from (B) by SDS–polyacrylamide gel electrophoresis (0.2 ml aliquot per lane, silver nitrate staining). P: protein extract (5 μg protein) obtained after partial purification of AKT1 C-Term (see Materials and methods). (**D**) Western blot analysis of the selected fractions (0.1 ml per lane) and of the total protein extract (P, 5 μg protein).

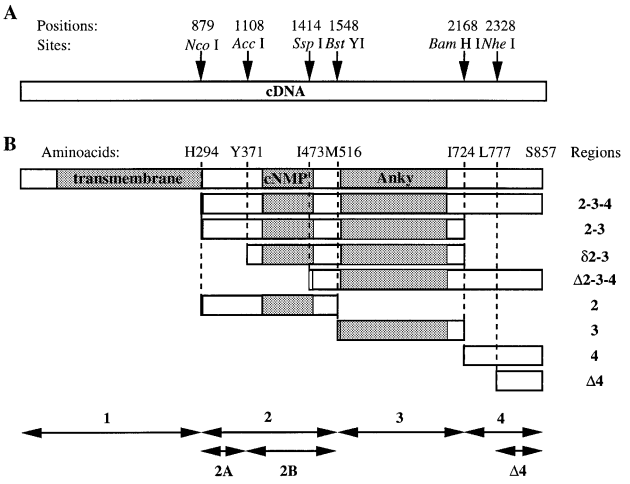

Fig. 3. Generation of *AKT1* cDNA fragments for testing intramolecular interactions in the two-hybrid system. (**A**) Positions of the restriction sites used for generating *AKT1* cDNA fragments. (**B**) Corresponding regions in the polypeptide sequence and nomenclature of individual regions. Domains identified by sequence homology data (Sentenac *et al*., 1992) are indicated by grey areas: the transmembrane domain (amino acids 61–295), the putative cyclic nucleotide-binding domain (cNMP, amino acids 393–477), and the ankyrin domain (anky, amino acids 522–693).

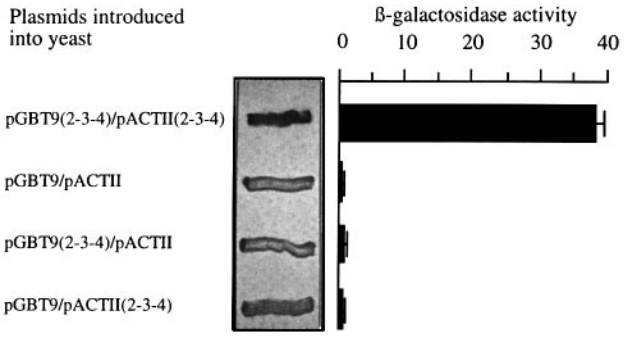

Fig. 4. Detection of the association of 2–3–4 polypeptides using the two-hybrid system. The yeast strain Y526 was transformed either with plasmids pGBT9(2–3–4) and pACTII(2–3–4), or with control couples of plasmids as indicated. Left, qualitative test on solid medium. Right, measurements of β-galactosidase activities (nmoles of ONPG hydrolysed per min per mg of protein). Mean values of three independent measurements, error bars denote standard deviations.

Constructs in pGBT9

Constructs in pACTII	E	2-3-4	2-3	Δ2-3-4	2	3	4	δ2-3	Δ4
E	**0.8**	0.6	0.4	0.7	0.5	0.7	0.3		
2-3-4	0.7	**38**	27	35	22.5	1	25	12.5	17.5
2-3	0.5	19	**14**		12.5		16.5		
Δ2-3-4	0.7	16		**0.9**			0.8	0.6	
2	0.4	13	13		**8**		8		7
3	0.5	0.9				**0.8**			
4	0.2	21	19	1	6.5		**0.7**	0.4	
δ2-3		14		0.2			0.9	**10**	0.7
Δ4		19.5			6			0.8	**0.8**

Fig. 5. Measurements of β-galactosidase activities in cell extracts of Y526 transformants. Yeast cells were electroporated in the presence of pGBT9 and pACTII plasmids containing either inserts corresponding to the indicated contructs (see Figure 3) or no insert (empty plasmid, E). β-galactosidase activities are expressed in nmoles of ONPG hydrolysed per min per mg of protein. Values shown are the mean of three independent experiments. Controls and negative results were less than or equal to one unit of β-galactosidase activity in all measurements. For positive results, standard deviations did not exceed 15% of the reported value.

coding for AKT1 C-Term was divided into three regions, called 2, 3 and 4 (Figure 3). Region 2 (amino acids H294–D517) comprises the putative cyclic nucleotide-binding domain (estimated from sequence homologies to include approximately amino acids 393–477) and adjacent sequences. Region 3 (M516–I724) includes the ankyrin repeat domain (amino acids 522–693), and region 4 (I724 to the last amino acid, S857) is the extreme C-terminus. Combinations of these structural elements, corresponding to regions 2–3–4 (complete C-Term sequence) and 2–3, were also investigated. In region 2, a segment (~100 amino acids) is present upstream from the putative cyclic nucleotide-binding domain. Cleavage of the 2–3 region cDNA sequence using the *Acc*I site resulted in a deletion covering most of this segment. The region (from Y371 to I724) corresponding to this truncated cDNA sequence was called δ2–3. The deleted sequence (amino acids H294–V370) was called 2A, and the rest of region 2, 2B (Figure 3). Similarly, using the *Ssp*I site in the sequence coding for the 2–3–4 region, another deletion was generated which led to the elimination of the sequence upstream from I473 (including the putative cyclic nucleotide-binding domain). The corresponding region was named Δ2–3–4. Finally, the *Nhe*I site present in the DNA sequence of region 4 was used to create region Δ4, comprising the last 81 amino acids (Figure 3).

In-frame fusions were made between cDNA sequences coding for GAL4 domains (DNA-binding or activator domain) and the cDNA fragments corresponding to the different regions described above. The vectors used, pGBT9 and pACTII, enable the synthesis of fusion proteins with either the DNA-binding domain or the activator domain of GAL4, respectively. Plasmids resulting from insertion of *AKT1* sequences downstream from that coding for the GAL4 domain were designated by the name of the vector followed by the region encoded by the cDNA fragment [e.g. pGBT9(2–3–4): pGBT9 containing the 2–3–4 coding sequence]. The recipient yeast strain was cotransformed with different combinations of plasmids as shown in Figures 4 and 5. The β-galactosidase activities were systematically detected by colorimetric tests on solid medium (example presented in Figure 4), and quantitative measurements were carried out after protein extraction. Control experiments were performed using empty plasmids in place of each one of the two plasmids. Confirmations of observed positive and negative reactions were obtained by testing the reciprocal combinations of plasmids (obtained by cloning the insert of plasmid pGBT9 in pACTII and reciprocally that of pACTII in pGBT9). In the case of positive results, such a reciprocity is considered as a strong argument for the existence of a true physical association (Allen *et al*., 1995).

Results obtained with the complete 2–3–4 region are presented in Figure 4. Control experiments using

pGBT9(2–3–4) and pACTII, or pGBT9 and pACTII(2–3–4) did not reveal any signal above the background level (0.8 unit of β-galactosidase activity) obtained with the combination pGBT9/pACTII. In contrast, yeast transformed with both plasmids pGBT9(2–3–4) and pACTII(2–3–4) turned blue rapidly (2 h) on X-Gal plates and displayed a high level of β-galactosidase activity. This result confirms that interactions occur between the AKT1 C-Term regions.

In order to identify which domains in the 2–3–4 region are able to bind to the complete 2–3–4 polypeptide sequence, regions 2, 3 and 4 were tested independently against 2–3–4. Regions 2 and 4 were found to be involved in intramolecular interactions (Figure 5). As expected from these results, regions 2–3 and Δ2–3–4 also interacted with region 2–3–4. No interaction could be detected with region 3.

In addition, each single region was tested against each of the others. Two identical region 2s exhibited a positive reaction in this assay. The β-galactosidase activity was ~5-fold lower than that observed with the complete 2–3–4 region, but clearly above the background level (Figure 5). Another interaction was detected between regions 2 and 4. The signals were significantly higher than those of the controls, and the two plasmid combinations gave similar levels of β-galactosidase activity (Figure 5). In agreement with these observations, the following couples of AKT1 fragments gave positive results: 2–3 and 2–3, 2–3 and 2, 2–3 and 4. In contrast, the negative results obtained with 4 and 4, or Δ2–3–4 and Δ2–3–4 suggest an absence of interaction between homologous 4 regions (Figure 5).

Deletions within the regions 2–3 and 4 leading to δ2–3 and Δ4 enabled the sequences that are more specifically involved in the interactions to be localized. As shown in Figure 5, the deletion in region 4 did not prevent association with region 2 (positive results with tests combining Δ4 and 2), showing that the extreme end of the protein is by itself able to bind to region 2. The region δ2–3 was still able to react with another δ2–3 but not with region 4; the 2A region is therefore required for association with the C-terminal end, but it is dispensable for the interaction between regions δ2–3. This interaction between two δ2–3 regions is lost when further 5′ sequence is deleted so that the cyclic nucleotide-binding domain is also removed, as a negative result is obtained with two Δ2–3–4 regions (Figure 5).

Discussion

Comparison of AKT1 channel structure with that of animal potassium channels

Two independent methods have been used to establish that the *AKT1* gene product is capable of self-association: the estimation of the native protein and C-Term molecular weights, and the determination of the binding properties of protein regions. Furthermore, from the molecular weights of the polypeptide complexes, it can be deduced that AKT1 shares the tetrameric organization common to the voltage-gated animal potassium channels of the Shaker family (Pongs, 1992; Caterall, 1995). This is the first demonstration of such a structure in a plant channel.

Although the overall structure of AKT1 is similar to that of voltage-gated animal channels, the mode of subunit assembly appears to be different, with a major role for the C-terminal domains in the case of AKT1. In channels of the Shaker family, the C-terminal cytoplasmic tail has been shown not to be involved in tetramerization (Li *et al.*, 1992; Hopkins *et al.*, 1994). AKT1 C-Term tetramers appear to be very stable, as the monomeric form is undetectable in gel filtration column eluates (Figure 2B). Thus, interactions involving the C-terminal hydrophilic part are likely to be important for AKT1 tetramerization. These results show that animal and plant potassium channels have developed independent ways to achieve their correct subunit assembly resulting in a tetrameric organization which is compatible with gating inside the channel pore.

Structural model

Using the two-hybrid system, we have defined two kinds of interactions: one between identical regions 2 (amino acids 294–516), and another one between region 2 and region Δ4 (amino acids L777 to the last one, S857). All the results obtained are consistent with the existence of these two interactions (Figure 5). They are reproducible and always reciprocal (i.e. the occurrence of a positive or negative result does not depend on the Gal4 domain with which the AKT1 fragments are fused, as demonstrated by the symmetry of measurements with respect to the diagonal of the table in Figure 5). In no combination did the ankyrin-repeat domain (included in region 3) show any interaction, either with itself or with other regions of AKT1 C-Term. Interaction with itself was not expected since ankyrin domains are known to interact with sequences which are not related to them (Hoffman, 1991). The negative results obtained with other parts of the molecule could be due to incorrect folding of the ankyrin domain when isolated from its normal polypeptide environment. However, the structure formed by the six adjacent ankyrin repeats would be expected to be globular and stable, from the data obtained on human erythrocyte ankyrin (Michaely and Bennett, 1993). Furthermore, negative results were obtained when region 3 was included in large parts of the molecule (see Δ2–3–4 with Δ2–3–4, and Δ2–3–4 with δ2–3 in Figure 5). Thus, the higher level of β-galactosidase activity that resulted in some cases when ankyrin domain was present (e.g. in tests with region 2–3 compared with the same tests performed with region 2) is likely to arise from an increased stability of the fusion protein and/or a better folding of the interacting domain, rather than from interactions involving ankyrin domains.

The two-hybrid experiments performed with region 2 revealed different binding properties between its N- and C-terminal segments. The first one (2A), was found to be involved in the interaction with the C-terminal end (Δ4) of the protein, whereas the other (2B, including the putative cyclic nucleotide-binding domain), appeared to be mainly responsible for the observed self-association of regions 2–3 (and consequently of region 2), since deletions of domain 2A or region 3 from region 2–3 (generating regions δ2–3 and 2, respectively) did not severely affect the interaction. Interestingly, in the *AKT1* gene (Basset *et al.*, 1995), two introns flank a segment corresponding to amino acids R323–L384. This provides further support for the hypothesis that the inserted sequence, corresponding for the junction between the transmembrane domain

and the putative cyclic nucleotide-binding domain, codes for a real domain.

Region 2B, which is likely to be involved in subunit tetramerization, is homologous to the cAMP-binding domain of cAMP-dependent protein kinases (Kaupp *et al*., 1989) and to the *E.coli* cAMP receptor protein (CRP) (Weber and Steitz, 1984). All these proteins are dimers. According to crystallography data, intersubunit contacts in the CRP protein are mainly found at the level of the C helix located downstream from the cAMP-binding domain (Weber *et al*., 1987). However, a proteolytic fragment which includes the N-terminal (cAMP-binding) domain, but lacks 85% of the C helix, is still able to form stable dimers (Heyduk *et al*., 1992). Studies concerning a cAMP-dependent protein kinase have shown that an isolated cAMP-binding domain expressed in *E.coli* is able to form dimers, and that the dimer displays a much higher nucleotide exchange rate than the monomer (Shabb *et al*., 1995). Similarly, interactions between cyclic nucleotide-binding domains could be involved in associations between AKT1 subunits.

Concerning the interactions involving domain 2A and region 4, the two-hybrid system does not predict whether they occur within a single polypeptide chain or between two different subunits. However, if they can occur between regions 2 and 4 of the same polypeptide, one would expect in a test involving regions 2–3–4 and 4, a competition between the two region 4s for binding to region 2. This does not appear to be the case, since the complete 2–3–4 sequence gives an even higher response than 2–3 when tested against region 4 in two-hybrid assays (Figure 5). We tend therefore to favour the hypothesis of inter-chain associations, attributing this preference to physical constraints preventing intra-chain folding. This interpretation is based on the assumption that the hybrid proteins containing region 4 alone are not favoured compared with those containing the complete 2–3–4 sequence, due to e.g. a higher stability.

According to our results, the interaction of the C-terminal ends of each subunit of the functional channel with the proximal regions of the C-Term regions would lead to the formation of four loops. This would result in an external localization of the four ankyrin domains that would favour interactions between these domains and as yet unidentified proteins. It is worth noting that in erythrocyte ankyrin, the 24 ankyrin repeats are thought to be folded in four globular domains of six ankyrin repeats each (Michaely and Bennett, 1993). The four six-repeat ankyrin domains of the AKT1 channel could form a similar structure.

Extension of the AKT1 structural model to other plant channels and to cyclic nucleotide-gated channels

All plant channels identified so far share high sequence homologies in the domains implicated, in this study, in intramolecular interactions: the cyclic nucleotide-binding domain and its junction with the hydrophobic domain (Cao *et al.*, 1995; Müller-Röber *et al.*, 1995), and region Δ4 (Figure 6). In AKT1 C-Term, these are the only regions which show sequence conservation between all plant channels of both the AKT1 and KAT1 types (presence and absence of an ankyrin domain, respectively); no homology can be found within sequences located between regions 2B and Δ4. We suggest therefore that the conserved sequences in regions 2 and Δ4 will play similar roles in all plant channels, and that the interactions responsible for channel tetramerization and protein folding involve common mechanisms. It is interesting that the ankyrin domain, which is specific to AKT1 family channels, was not found to be involved in interactions within AKT1.

Like potassium channels, cyclic nucleotide-gated cation channels are thought to be multimeric (Eismann *et al.*, 1993), probably tetrameric (Gordon and Zagotta, 1995; Liu *et al*., 1996). They can function either as homomultimers of α subunits or as heteromultimers combining homologous α and β subunits (Chen *et al*., 1993; Korschen *et al*., 1995). Apart from homologies in the hydrophobic domain, all known α and β subunits share 22 to 25% identity [Fasta program (Pearson and Lipman, 1988), data not shown] with AKT1 throughout the region extending from T336 to V445 in AKT1 (end of region 2A + putative cyclic nucleotide-binding domain). Thus, subunit assembly in cyclic nucleotide-gated channels might be mediated, at least in part, by sequences homologous to this AKT1 segment. While looking for equivalents of region Δ4 in cyclic nucleotide-gated channels, we found a weak homology (38% identity in a 21 amino acid overlap) with the C-terminal end of some β subunits sequences (Figure 6).

In conclusion, we propose a global structural organization, very different from that of animal voltage-gated potassium channels, which would be common to all known plant potassium channels. To define the exact contribution of C-terminal ends in the tetramer more precisely, a detailed structural analysis of the crystallized protein will probably be required. Further investigations will also be needed to test whether the plant channel model can be extended to cyclic nucleotide-gated channels. However, the similarity of primary structure organization suggests that these channels could adopt a mode of assembly partly analogous to that of AKT1, with the participation of the C-terminal intracytoplasmic tail, specifically in the region including the cyclic nucleotide-binding domain.

Materials and methods

Expression of cDNA products in insect cells

*Sf*9 and *Sf*21 cell lines were propagated as described by Gaymard *et al.* (1996). The two recombinant transfer vectors, harbouring *AKT1* cDNA or the cDNA sequence coding for AKT1 C-Term, were derived from pGmAc34T (Davrinche *et al*., 1993). The insertion of *AKT1* cDNA into pGmAc34T has been described previously (Gaymard *et al*., 1996). The sequence coding for AKT1 C-Term was introduced into pGmAc34T–*Sma*I. This vector was created from pGmAc34T by insertion of a *Sma*I site at position +45 (from the ATT triplet replacing the ATG initiation codon of the polyhedrin gene). The partial *AKT1* cDNA sequence was obtained from plasmid pUC9–AKT1, containing the *Not*I *AKT1* fragment from pHS41 (Sentenac *et al*., 1992) inserted at a *Not*I site previously introduced into the pUC9 polylinker. This plasmid was digested at the *Nco*I site present at the end of the S6 segment, blunt-ended with the Klenow fragment of *E.coli* DNA polymerase I, and religated. This created an ATG codon and an *Nsi*I site. An *Nsi*I–*Sma*I fragment encoding AKT1 C-Term was isolated by partial *Nsi*I digestion and use of the *Sma*I site of the pUC9 polylinker. This fragment was cloned into pJRD184 (Heusterspreute *et al*., 1985) using the *Nsi*I and *Sma*I sites of this vector. *Sma*I sites were introduced at both ends of the cDNA sequence by subcloning firstly into pSP72 (Promega), using *Bgl*II and *Sma*I sites, and then into pBluescript SKII (Stratagene), using *Bgl*II and

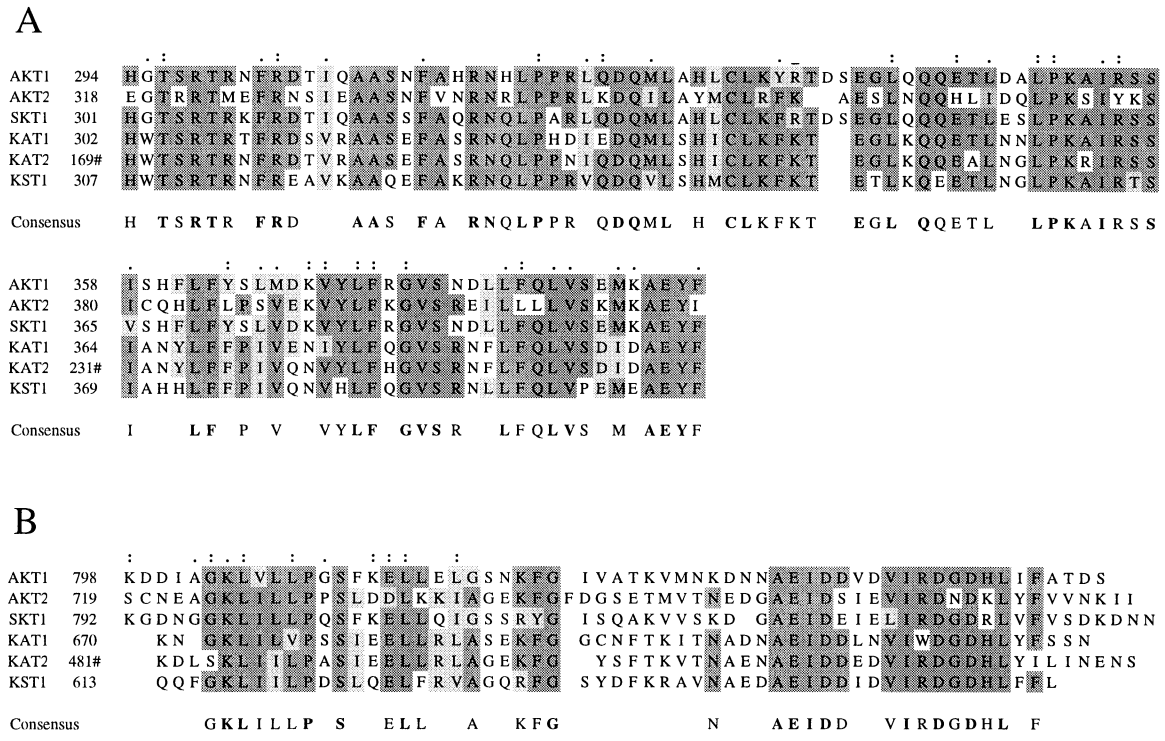

Fig. 6. Sequence homologies between potassium channels. (**A**) Sequence corresponding to the junction region linking the transmembrane domain to the putative cyclic nucleotide-binding domain (amino acids 294–392 in AKT1). (**B**) C-terminal end (amino acids 798–857 in AKT1). Dark grey boxed letters: amino acids conserved in at least four sequences. Light grey: conservative changes. (#) indicates that the numbering does not begin at the first amino acid, as the complete cDNA sequence is unavailable. (:): amino acids conserved between AKT1 and β subunits of mammalian cyclic nucleotide-gated channels: hRCNC2 (Chen *et al*., 1993), X89626 (Korschen *et al*., 1995), CNG4c, CNG4d and CNG4e (Biel *et al*., 1996). (.): conservative changes (see above).

*Xho*I sites. The *Sma*I fragment containing the AKT1 partial cDNA sequence was then introduced into pGmAc34T–*Sma*I.

Sf21 cells were transfected with wild-type viral DNA and the recombinant transfer vectors (Davrinche *et al.*, 1993). Recombinant baculoviruses were purified, and amplified in *Sf*9 cells to 10^8 p.f.u./ml for protein production.

Preparation of protein extracts

*Sf*9 cell extracts were prepared according to Gaymard *et al.* (1996). AKT1 was solubilized from the microsomal fraction (100 000 *g* pellet) with lysophosphatidylcholine [ratio detergent/protein of 5 (w/w), in grinding medium minus glycerol and leupeptin]. AKT1 C-Term was extracted following the same protocol as for AKT1, except that after 1 h centrifugation at 100 000 *g* it was obtained in the soluble protein fraction. Both polypeptides were partially purified by anion exchange chromatography (Mono-Q, Pharmacia). The elution buffer contained 10% glycerol, 1 mM EDTA and either 20 mM histidine, pH 8 plus 0.05% lysophosphatidylcholine (for AKT1) or 20 mM piperazine, pH 9 (for AKT1 C-Term). Proteins were eluted using a NaCl step gradient from 0 to 1 mol/l, with steps of 0.1 mol/l.

Size-exclusion chromatography

A 250 ml Sephacryl S-300 column (Pharmacia) was equilibrated (200 µl/min) with either 20 mM bis–tris propane–HCl pH 7 buffer, containing 100 mM NaCl, 1 mM EDTA, 10% glycerol and 0.05% lysophosphatidylcholine for AKT1, or 20 mM piperazine pH 9 buffer, containing 100 mM NaCl, 1 mM EDTA and 10% glycerol for AKT1 C-Term. The elution was carried out in the same buffer, after loading 100 µg of protein. Columns were calibrated with molecular weight standards from Sigma (MW-GF-1000): carbonic anhydrase (29 kDa), bovine serum albumin (66 kDa), alcohol dehydrogenase (150 kDa), β-amylase (200 kDa), apoferritin (443 kDa) and thyroglobulin (669 kDa).

Immunoblots

Polyclonal antibodies were raised against the C-terminal region of AKT1, as described by Gaymard *et al.* (1996). Elution fractions from the size-exclusion columns were analysed by dot blots, a 1 µl aliquot of each fraction being deposited onto a nitrocellulose membrane (Sartorius). For Western blot analyses, proteins were separated by SDS–PAGE according to Laemmli (1970) and electroblotted to a nitrocellulose membrane (Sartorius) at 100 V for 1 h in a medium containing 25 mM Tris, 192 mM glycine, 0.1% SDS and 20% methanol.

Membranes were processed as described by Gaymard *et al.* (1996). AKT1 or AKT1 C-Term were detected by chemiluminescence (Aurora kit, ICN). For the dot blot quantifications, intensities of the spots were measured by densitometry using 'The Imager^{TM}' (Appligene) and the NIH-Imager program.

Two-hybrid constructions

Plasmid vectors pGBT9 (Bartel and Fields, 1995) and pACTII [derived from pACT (Durfee *et al*., 1993) and kindly provided by S.Elledge, Baylor college of Medicine, Houston, TX] were used for the generation of fusion proteins with the DNA-binding domain and the activator domain of GAL4, respectively.

In-frame fusions were made between the DNA-binding or activator domain of GAL4 and fragments from *AKT1* cDNA in pHS41 (Sentenac *et al.*, 1992). Cloning procedures involved DNA digestions at appropriate restriction sites (see Figure 3), end modifications using the Klenow fragment of DNA polymerase I, and intermediate subclonings into pBluescript SKII (Stratagene). All constructions were checked by DNA sequencing of the vector–insert junction region.

Yeast transformation

All constructions were introduced into strain Y526 (Mata, *ura3-52, his3-200, ade2-101, lys2-801, trp1-901, leu2-3, 112, canr, gal4-542, gal80-538, URA3::Gal1–lacZ*) (Bartel and Fields, 1995). Yeast were routinely grown on YPD medium (Sherman, 1991). For transformation, an exponential phase culture (0.6 absorbance unit) was pelleted by centrifugation, and resuspended in 1/20 culture volume of YPD medium supplemented with DTT (25 mM) and HEPES (20 mM, pH 8). After a 30 min incubation at 30°C under constant agitation, cells were washed twice with EB buffer (10 mM Tris, 270 mM sucrose, 1 mM $MgCl_2$, pH 8) and resuspended in 1/50 culture volume of EB buffer. Fifty microlitre aliquots of the yeast suspension were mixed with 1 µg of each plasmid, and deposited between two plate electrodes (type D03N, Jouan, Saint Herblain, France). Plasmids were introduced into yeast cells

by electroporation with a Jouan GHT 1287B apparatus, by a 12 ms pulse at 725 V. After transformation, yeast cells were plated onto a selective medium lacking leucine and tryptophan, composed of SD minimal medium (Sherman, 1991), complemented with isoleucine (30 mg/l), valine (150 mg/l), adenine (20 mg/l), arginine (20 mg/l), histidine (20 mg/l), lysine (30 mg/l), methionine (20 mg/l), phenylalanine (50 mg/l), threonine (200 mg/l), tyrosine (30 mg/l) and uracil (20 mg/l).

Assay for reporter gene expression

Transformed yeast were replicated onto selective medium containing raffinose (2%) in place of glucose, incubated for 3 days at 30°C and tested for β-galactosidase activity directly on the agarose plate, as described by Werner *et al*. (1993). Quantitative tests were performed after protein extraction, according to Bartel and Fields (1995), using *o*-nitrophenyl-β-D-galactopyranoside (ONPG) as substrate.

Acknowledgements

We are grateful to Helen Logan for critical reading of the manuscript. Our work is partly supported by the Bio Avenir programme (funded by Rhône-Poulenc and the French Ministry in charge of Research and Industry) and by the European Communities' BIOTECH Programme (Project of Technological Priority 1993–1996)

References

Allen,J.B., Walberg,M.W., Edwards,M.C. and Elledge,S.J. (1995) Finding prospective partners in the library: the two-hybrid system and phage display find a match. *Trends Biochem. Sci.*, **20**, 511–516.

Anderson,J.A., Huprikar,S.S., Kochian,L.V., Lucas,W.J. and Gaber,R.F. (1992) Functional expression of a probable *Arabidopsis thaliana* potassium channel in *Saccharomyces cerevisiae*. *Proc. Natl Acad. Sci. USA*, **89**, 3736–3740.

Attali,B. *et al*. (1993) Multiple mRNA isoforms encoding the mouse cardiac Kv1.5 delayed rectifier K^+ channel. *J. Biol. Chem.*, **268**, 24283–24289.

Babila,T., Moscucci,A., Wang,H., Weaver,F. and Koren,G. (1994) Assembly of mammalian voltage-gated potassium channel: evidence for an important role of the first transmembrane segment. *Neuron*, **12**, 615–626.

Bartel,P.L. and Fields,S. (1995) Analysing protein-protein interactions using two-hybrid system. *Methods Enzymol.*, **254**, 241–263.

Basset,M., Conéjéro,G., Lepetit,M., Fourcroy,P. and Sentenac,H. (1995) Organization and expression of the gene coding for the potassium transport system AKT1 of *Arabidopsis thaliana*. *Plant Mol. Biol.*, **29**, 947–958.

Biel,M., Zong,X., Ludwig,A., Sautter,A. and Hofmann,F. (1996) Molecular cloning and expression of a modulatory subunit of the cyclic nucleotide-gated cation channel. *J. Biol. Chem.*, **271**, 6349–6355.

Cao,Y. *et al*. (1995) Multiple genes, tissue specificity, and expression-dependent modulation contribute to the functional diversity of potassium channels in *Arabidopsis thaliana*. *Plant Physiol.*, **109**, 1093–1106.

Caterall,W.A. (1995) Structure and function of voltage-gated ion channels. *Annu. Rev. Biochem.*, **64**, 493–531.

Chen,T.Y., Peng,Y.W., Dhallan,R.S., Ahamed,B., Reed,R.R. and Yau,K.W. (1993) A new subunit of the cyclic nucleotide-gated cation channel in retinal rods. *Nature*, **362**, 764–767.

Davrinche,C., Pasquier,C., Cerutti,M., Serradell,L., Clément,D., Devauchelle,G., Michelson,S. and Davignon,J.L. (1993) Expression of human cytomegalovirus immediate early protein IE1 in insect cells: splicing of RNA and recognition by $CD4^+$ T^-cell clones. *Biochem. Biophys. Res. Commun.*, **195**, 469–477.

Durfee,T., Becherer,K., Chen,P.L., Yeh,S.H., Yang,Y., Kilburn,A.E., Lee,W.H. and Elledge,S.J. (1993) The retinoblastoma protein associates with the protein phosphatase type 1 catalytic subunit. *Genes Dev.*, **7**, 555–569.

Eismann,E., Bönigk,W. and Kaupp,U.B. (1993). Structural features of cyclic nucleotide-gated channels. *Cell Physiol. Biochem.*, **3**, 332–351.

Gaymard,F. *et al*. (1996) The baculovirus/insect cell system as an alternative to *Xenopus* oocytes. *J. Biol. Chem.*, **271**, 22863–22870.

Gordon,S.E. and Zagotta,W.N. (1995) Subunit interactions in coordination of Ni^{2+} in cyclic nucleotide-gated channels. *Proc. Natl Acad. Sci. USA*, **92**, 10222–10226.

Heusterspreute,M., Thi,V.H., Emery,S., Tournis-Gamble,S., Kennedy,N. and Davison,J. (1985) Vectors with restriction site banks IV. pJRD184, a 3793-bp vector having 43 unique cloning sites. *Gene*, **39**, 299–304.

Heyduk,E., Heyduk,T. and Lee,J.C. (1992) Intersubunit communications in *Escherichia coli* cyclic AMP receptor protein: studies of the ligand-binding domain. *Biochemistry*, **31**, 3682–3688.

Hoffman,M. (1991) New role found for a common protein 'motif'. *Science*, **253**, 742.

Hopkins,W.F., Demas,V. and Tempel,B.L. (1994) Both N- and C-terminal regions contribute to the assembly and functional expression of homo- and heteromultimeric voltage-gated K^+ channels. *J. Neurosci.*, **14**, 1385–1393.

Isacoff,E.Y., Jan,Y.N. and Jan,L.Y. (1990) Evidence for the formation of heteromultimeric potassium channels in *Xenopus* oocytes. *Nature*, **345**, 530–534.

Jan,L.Y. and Jan,Y.N. (1992) Tracing the roots of ion channels. *Cell*, **69**, 715–718.

Kaupp,U.B. *et al*. (1989) Primary structure and functional expression from complementary DNA of the rod photoreceptor cyclic GMP-gated channel. *Nature*, **342**, 762–766.

Ketchum,K.A. (1996) Isolation of an ion channel gene from *Arabidopsis thaliana* using the H5 signature sequence from voltage-dependent K^+ channels. *FEBS Lett.*, **378**, 19–26.

Kirsch,G.E., Drewe,J.A., De Biasi,M., Hartmann,H.A. and Brown,A.M. (1993) Functional interactions between K+ pore residues located in different subunits. *J. Biol. Chem.*, **268**, 13799–13804.

Korschen,H.G. *et al*. (1995) A 240 kDa protein represents the complete beta subunit of the cyclic nucleotide-gated channel from rod photoreceptor. *Neuron*, **15**, 627–636.

Laemmli,U.K. (1970) Cleavage of structural proteins during the assembly of the head of bacteriophage T4. *Nature*, **227**, 680–685.

Lagarde,D., Basset,M., Lepetit,M., Conéjéro,G., Gaymard,F., Astruc,S. and Grignon,C. (1996) Tissue-specific expression of *Arabidopsis* AKT1 gene is consistent with a role in K^+ nutrition. *Plant J.*, **9**, 195–203.

Lee,T.E., Philipson,L.H., Kuznetsov,A. and Nelson,D.J. (1994) Structural determinant for assembly of mammalian K^+ channels. *Biophys. J.*, **66**, 667–673.

Li,M., Jan,Y.M. and Jan,Y.M. (1992) Specification of subunit assembly by the hydrophilic amino-terminal domain of the Shaker potassium channel. *Science*, **257**, 1225–1230.

Li,M., Unwin,N., Stauffer,K.A., Jan,Y.N. and Jan,L.Y. (1994) Images of purified Shaker potassium channels. *Curr. Biol.*, **4**, 110–115.

Liman,E.R., Tytgat,J. and Hess,P. (1992) Subunit stoichiometry of a mammalian K^+ channel determined by construction of multimeric cDNAs. *Neuron*, **9**, 861–871.

Liu,D.T., Tibbs,G.R. and Siegelbaum,S.A. (1996) Subunit stoichiometry of cyclic nucleotide-gated channels and effects of subunit order on channel function. *Neuron*, **16**, 983–990.

Lux,S.E., John,K.M. and Bennett,V. (1990) Analysis of cDNA for human erythrocyte ankyrin indicates a repeated structure with homology to tissue-differentiation and cell-cycle control proteins. *Nature*, **344**, 36–42.

MacKinnon,R. (1991) Determination of the subunit stoichiometry of a voltage-activated potassium channel. *Nature*, **350**, 232–235.

Michaely,P. and Bennett,V. (1992) The ANK repeat: a ubiquitous motif involved in macromolecular recognition. *Trends Cell Biol.*, **2**, 127–129.

Michaely,P. and Bennett,V. (1993) The membrane-binding domain of ankyrin contains four independently folded subdomains, each comprised of six ankyrin repeats. *J. Biol. Chem.*, **268**, 22703–22709.

Müller-Röber,B., Ellenberg,J., Provart,N., Willmitzer,L., Busch,H., Becker,D., Dietrich,P., Hoth,S. and Hedrich,R. (1995) Cloning and electrophysiological analysis of KST1, an inward rectifying K^+ channel expressed in potato guard cells. *EMBO J.*, **14**, 2409–2416.

Pearson,W.R. and Lipman,D.J. (1988) Improved tools for biological sequence comparison. *Proc. Natl Acad. Sci. USA*, **85**, 2444–2448.

Peled,H. and Shai,Y. (1993) Membrane interaction and self-assembly within phospholipid membranes of synthetic segment corresponding to the H-5 region of the shaker K^+ channel. *Biochemistry*, **32**, 7879–7885.

Pfaffinger,P.J. and DeRubeis,D. (1995) Shaker K^+ channel T1 domain self-tetramerizes to a stable structure. *J. Biol. Chem.*, **270**, 28595–28600.

Pongs,O. (1992) Molecular biology of voltage-dependent potassium channels. *Physiol. Rev.*, **72**, S69–S88.

Ruppersberg,J.P., Schröter,K.H., Sakmann,B., Stocker,M., Sewing,S. and Pongs,O. (1990) Heteromultimeric channels formed by rat brain potassium channel proteins. *Nature*, **345**, 535–537.

Sentenac,H., Bonneaud,N., Minet,M., Lacroute,F., Salmon,J.M., Gaymard,F. and Grignon,C. (1992) Cloning and expression in yeast of a plant potassium ion transport system. *Science*, **256**, 663–665.

Shabb,J.B., Poteet,C.E., Kapphahn,M.A., Muhonen,W.M., Baker,N.E. and Corbin,J.D. (1995) Characterization of the isolated cAMP-binding B domain of cAMP-dependent protein kinase. *Protein Sci.*, **4**, 2100–2106.

Shen,N.V., Chen,X., Boyer,M.M. and Pfaffinger,P.J. (1993) Deletion analysis of K^+ channel assembly. *Neuron*, **11**, 67–76.

Shen,N.V. and Pfaffinger,P.J. (1995) Molecular recognition and assembly sequences involved in the subfamily-specific assembly of voltage-gated K^+ channel subunit proteins. *Neuron*, **14**, 625–633.

Sherman,F. (1991) Getting started with yeast. *Methods Enzymol.*, **194**, 3–20.

Tu,L., Santarelli,V. and Deutsch,C. (1995) Truncated K^+ channel DNA sequences specifically suppress lymphocyte K^+ channel gene expression. *Biophys. J.*, **68**, 147–156.

Tu,L., Santarelli,V., Sheng,Z., Skach,W., Pain,D. and Deutsch,C. (1996) Voltage-gated K^+ channels contain multiple intersubunit association sites. *J. Biol. Chem.*, **271**, 18904–18911.

Van Dongen,A.M., Frech,G.C., Drewe,J.A., Joho,R.H. and Brown,A.M. (1990) Alteration and restoration of K^+ channel function by deletions at the N- and C-termini. *Neuron*, **5**, 433–443.

Weber,I.T. and Steitz,T.A. (1984) Model of specific complex between catabolite gene activator protein and B-DNA suggested by electrostatic complementarity. *Proc. Natl Acad. Sci. USA*, **81**, 3973–3977.

Weber,I.T., Steitz,T.A., Bubis,J. and Taylor,S.S. (1987) Predicted structures of cAMP binding domains of type I and II regulatory subunits of cAMP-dependent protein kinase. *Biochemistry*, **26**, 343–351.

Werner,M., Chaussivert,N., Willis,I.M. and Sentenac,A. (1993) Interaction between a complex of RNA polymerase III subunits and the 70-kDa component of transcription factor IIIB. *J. Biol. Chem.*, **268**, 20721–20724.

Wes,P.D., Chevesich,J., Jeromin,A., Rosenberg,C., Stetten,G. and Montell,C. (1995) TRPC1, a human homolog of a *Drosophila* store-operated channel. *Proc. Natl Acad. Sci. USA*, **92**, 9652–9656.

Xu,J., Yu,W., Jan,Y.N., Jan,L.Y. and Li,M. (1995) Assembly of voltage-gated potassium channels. *J. Biol. Chem.*, **270**, 24761–24768.

Zufall,F., Firestein,S. and Shepherd,G.M. (1994) Cyclic nucleotide-gated ion channels and sensory transduction in olfactory receptor neurons. *Annu. Rev. Biophys. Biomol. Struct.*, **23**, 577–607.

Received on January 17, 1997; revised on March 20, 1997